Direct ink writing of catalytically active UiO-66 polymer composites

Adam J. Young, [#a] Remy Guillet-Nicolas, [#b] Ellis S. Marshall,[a] Freddy Kleitz,[b] Alex J. Goodhand,[a] Lloyd B.L. Glanville,[a] Michael R. Reithofer*[c] and Jia Min Chin*[ac]

[a] *Faculty of Science and Engineering, Chemistry, University of Hull, Cottingham Road, Kingston upon Hull, HU6 7RX, UK. E-mail: j.chin@hull.ac.uk*

[b] *Department of Inorganic Chemistry – Functional Materials, Faculty of Chemistry, University of Vienna, Währinger Straße 42, 1090 Vienna, Austria*

[c] *Department of Inorganic Chemistry, Faculty of Chemistry, University of Vienna, University of Vienna, Währinger Straße 42, 1090 Vienna, Austria. E-mail: michael.reithofer@univie.ac.at*

[#] *These authors contributed equally.*

Table of Contents

1. Definition of terms

UiO-66 composite (UiO-66comp): The sample is formulated in accordance to the description in section 1.4 in this ESI, and photocured by UV light at 365 nm. No post-treatment has been carried out.

UiO-66 composite post furnace (UiO-66comp$_{\Delta}$): The UiO-66 composite (*see above*) which has been subjected to 280 °C for 30 minutes in an open-air furnace, then left to cool to room temperature on the benchtop. The sample is then washed with dichloromethane (DCM) and dried *in vacuo* at 50 °C overnight.

UiO-66 composite post furnace, hydrated **(UiO-66comp$_{\Delta\cdot hyd}$)**: UiO-66comp$_{\Delta}$**,** soaked in water for 24 hours, washed with water and DCM, dried *in vacuo* at 50 °C overnight.

UiO-66 MOF: The synthesised UiO-66 MOF as described in section 1.2.

UiO-66 MOF$_{\Delta}$: UiO-66 MOF, subjected to 280 °C for 30 minutes in an open-air furnace, then left to cool to room temperature on the benchtop.

UiO-66 MOF$_{\Delta\cdot hyd}$: UiO-66 MOF$_{\Delta}$ was soaked in water for 24 hours and washed with DCM, dried *in vacuo* at 50 °C overnight.

UiO-66 composite ink: The formulated mixture as per section 1.4 prior to irradiation with 365 nm UV light.

Polymer binder mixture (acrylates): Ebecryl® 8413 (3.27 g) and trimethylolpropane propoxylate triacrylate (TMPPTA) (0.962 g) mixed together.

PI mixture: The 80:20 weight percent mixture of 2-hydroxy-2-methylpropiophenone and phenylbis (2,4,6-trimethylbenzoyl) phosphine oxide.

Resin mixture: Polymer binder mixture (as above) with PI mixture.

2. Experimental

2.1. Reagents, materials and equipment

Zirconium chloride was purchased from Alfa Aesar. Terephthalic acid, methyl paraoxon and trimethylolpropane propoxylate triacrylate, M_n 644 (TMPPTA) were purchased from Sigma Aldrich. *N*,*N*-dimethylformamide (DMF) was purchased from Merck. Hydrochloric acid, dichloromethane and absolute ethanol were purchased from VWR international. Ebecryl® 8413 was supplied by Allnex. The photoinitiators, 2-hydroxy-2-methylpropiophenone and phenylbis(2,4,6-trimethylbenzoyl) phosphine oxide were purchased from TCI Chemicals. *N*-ethylmorpholine and deuterated water (D_2O) were purchased from Fluorochem. All chemicals were used as received.

A Velleman K8200 3D printer was purchased from Vellemen.com along with a commercially available paste extruder from the same supplier. The freeware Repetier k8200 host utilized is free of charge, and available online. Objects were designed using TinkerCAD, sliced using Cura 15.04.6 and exported in GCode.

A 5 meter UV light strip (12 V, 395-405 nm) was purchased from AMARS, and a 50 W 365-370 nm LED was purchased from Wholesale LEDs, China.

2.2. Synthesis

UiO-66 was synthesized in an adaptation of referenced literature procedure.[1] Zirconium chloride (5.7 g, 0.54 mmol), DMF (206 mL) and hydrochloric acid (46 mL, 37 %) were placed in a 1 L Schott bottle and sonicated until fully dissolved. Terephthalic acid (5.7 g, 0.75 mmol) was solubilized in DMF (481 mL) by sonication before being added to the zirconium chloride solution and vortexed for 5 min for mixing.

The bottle was sealed and placed in a preheated 80 °C oven for 16 h. The white solid was collected by filtration and washed with DMF (30 mL x 2) and subsequently ethanol (30 mL x 3). The solid was left to dry overnight in a 50 °C oven. To activate the MOF, powdered UiO-66 was heated at 150 °C and placed under a high vacuum for 4 hours.

2.2.1. Preparation of photoinitiator (PI) blend

The photoinitiator (PI) blend was prepared by dissolving (via ultrasound bath) phenylbis(2,4,6-trimethylbenzoyl) phosphine oxide (0.5 g, 1.19 mmol) in 2-hydroxy-2-methylpropiophenone (2.0 g, 12.18 mmol).

2.2.2. Preparation of UiO-66 ink

UiO-66 particles (5.0 g) were dispersed in a minimum amount of ethanol (7.5 mL), by means of sonication for 30 min. Afterwards the suspension was filled into a 25 mL Luer lock plastic syringe and the PI blend (0.38 g) was added and homogenized. To this mixture, Ebecryl® 8413 (3.27 g) and trimethylolpropane propoxylate triacrylate (TMPPTA) (0.962 g) were added and homogenized using

an Ultra Turrax T18 mixer at 10,000 rpm for 3 min. The final ink was sealed and protected from light and stored at RT until used (within 3 hours).

2.2.3. 3D printing of UiO-66 composite

The UiO-66 ink was loaded into a 25 mL Luer lock plastic syringe fitted with a 16-gauge PTFE Luer lock needle. The syringe was positioned into the Velleman K8200 3D printer modified with a paste extruder. The 3D printer was placed in a plastic casing through which a gentle stream of N_2 was flowed to decrease oxygen inhibition of polymer curing. G-code was created for the desired prints and loaded onto K8200 Repetier-Host software, connected to the 3D printer. The sample was irradiated with 365 nm UV light during printing. The printed samples were then kept under UV irradiation for 3 minutes for post-curing.

2.2.4. Thermal treatment of UiO-66 3DP composite

3D printed samples were placed in a high purity alumina crucible and placed into a preheated furnace at 280 °C for 30 min. The furnaced samples were then taken out and allowed to cool to room temperature before being washed with dichloromethane (DCM) and placed in a vacuum oven at 50 °C overnight. The MOF content of the resultant samples was found to be 91 wt.% based on ICP-OES and TGA.

2.2.5. Catalysis of methyl-paraoxon hydrolysis

Hydrolysis experiments were carried out at room temperature. A solid sample of UiO-66 MOF (activated overnight *in vacuo* at 150 °C, 2.5 mg, 6 mol.%), UiO-66 MOF_{Δ} (2.5 mg, 6 mol.%), UiO-66 $MOF_{\Delta\cdot hyd}$ (2.5 mg, 6 mol.%), UiO-66$comp_{\Delta}$ (3.4 mg, 73 wt.% of MOF, 6 mol.% catalyst) or UiO-66$comp_{\Delta\cdot hyd}$ (3.4 mg, 73 wt.% of MOF, 6 mol.% catalyst) was added to an aqueous solution of *N*-ethylmorpholine buffer (0.45 M in 10% D_2O/H_2O, 1 mL) and shaken for 5 min. Dimethyl paraoxon solution (4 µL) was then added to the MOF suspension. The mixture was vigorously shaken for 10 seconds. The sample was transferred to an NMR tube whereby the catalysis was monitored *in-situ* by $^{31}P\{^1H\}$-NMR. The progress of the reaction was monitored with 3 min increments for the first 60 minutes, then 6-minute increments for the following 60 min and a final reading at an increment at 200 minutes. Control experiments were conducted in an identical manner but in the absence of MOF material (background hydrolysis of agent).

3. Characterisation

SEM images were captured on a Cambridge Instruments Stereoscan 360 SEM model running at 20 kV. All samples were gold sputter coated prior to analysis.

Fourier-transform infrared attenuated total reflectance (FTIR-ATR) spectroscopy was carried out on a Thermoscientific Nicolet iS5 fitted with a Pike Miracle diamond ATR attachment. 6 scans were collected and averaged for samples, with background subtraction.

N2 adsorption/desorption isotherm measurements at -196 °C were performed using an Autosorb-iQ2-MP sorption instrument (Quantachrome Instruments, Boynton Beach, FL, USA). Prior to the measurements, samples were outgassed under vacuum at 150 °C for 12 h, unless otherwise indicated. The UiO-66comp sample was also outgassed under vacuum at 100 °C for 12 h. Apparent BET specific surface area, SBET, was determined via the BET equation using the Rouquerol et al. procedure for microporous adsorbents,35 and total pore volume was obtained at P/P0 = 0.95 using the Gurvitch rule. Relevant pore size distribution was obtained from the adsorption branch of the isotherms by applying the kernel of (metastable) NLDFT adsorption isotherms, considering a polar surface and a cylindrical pore model.30 NLDFT micropore volume was determined using the same kernel. For comparison purpose, the micropore volumes were additionally determined using the t-plot method in the range 0.15≤ P/P0 ≤ 0.4. The calculations were carried out using the ASiQWin software 5.0 provided by Quantachrome Instruments.

Thermogravimetric analysis (TGA) was performed using a Perkin Elmer TGA 4000 instrument in the temperature range of 30 – 700 °C with a heating rate of 10 °C·min-1 under a 30 mL·min-1 air flow.

Powder X-ray diffraction (PXRD) was performed on a PAN analytical Empyrean Series 2 Diffractometer operating CuKα1 (λ = 1.54056 Å). Prior to analysis all samples were dried and then crushed by pestle and mortar and loaded into the PXRD sample holder.

NMR spectra were recorded on a JEOL ECZ 400S spectrometer, 31P{1H}-NMR spectra were recorded at 162.0 MHz and referenced externally to H3PO4 P = 0 ppm. Chemical shifts are given in ppm ().

Rheological data were collected at 20 °C with a Bohlin rheometer fitted with a PP40 parallel plate.

ICP-OES analysis was performed on a Perkin Elmer Optima 5300DV ICP-OES spectrometer and was calibrated against 10 ppm standards and externally calibrated with a certified reference digest (CRM-ES).

Mechanical testing was conducted on a Mark-10 Model DC4060 mechanical testing instrument with a Force Gauge Model M5-500 attachment to assess the mechanical integrity of the 3D-printed MOF composites. After cutting, the samples were placed between two metal plates and compressed with 1400 N load cell travelling at 2.4 $mm \cdot min^{-1}$ while the

applied load and piston movement were recorded. The compressive force was applied in the axial direction until the monoliths broke.

3.1. Scanning Electron Microscopy, SEM

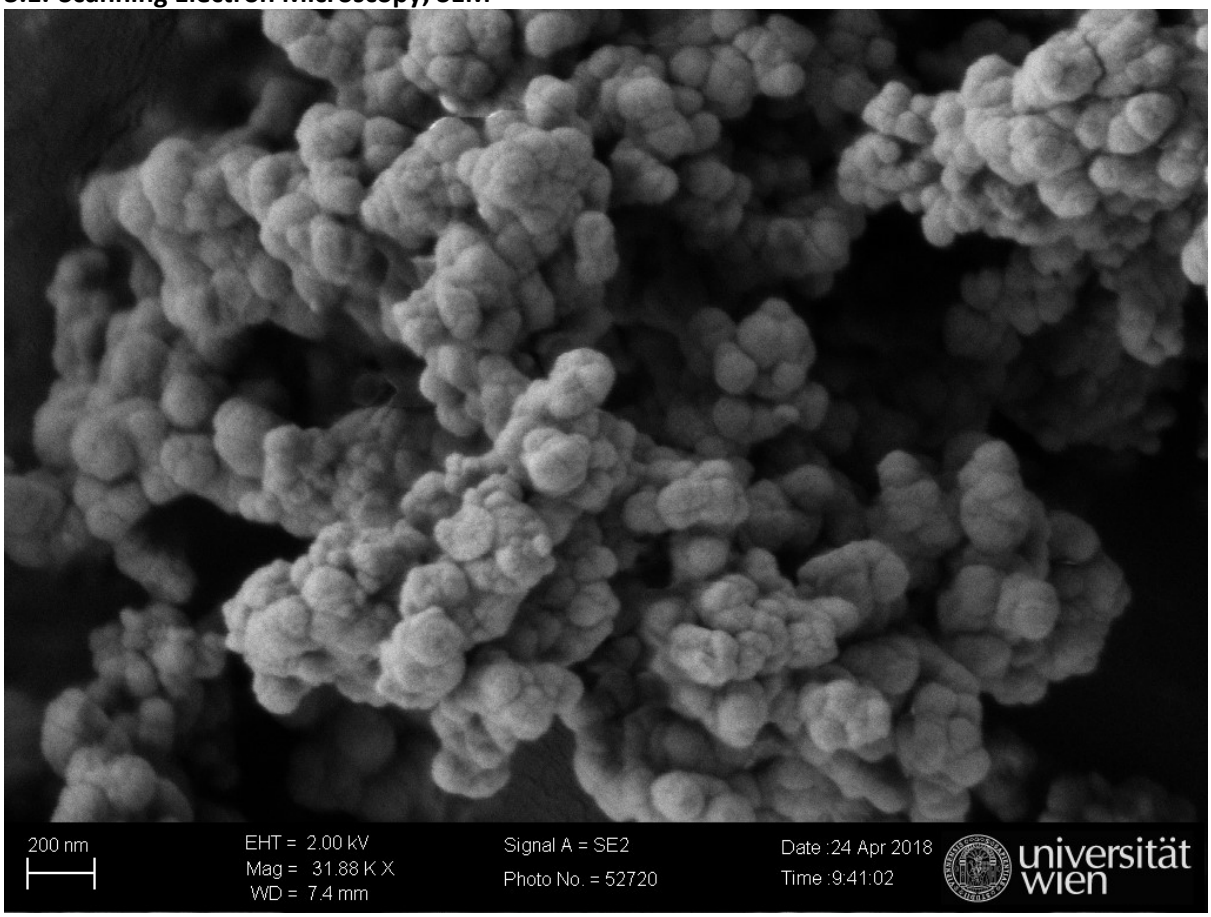

Figure S1. SEM image of UiO-66 MOF particles.

3.2. Rheological measurements

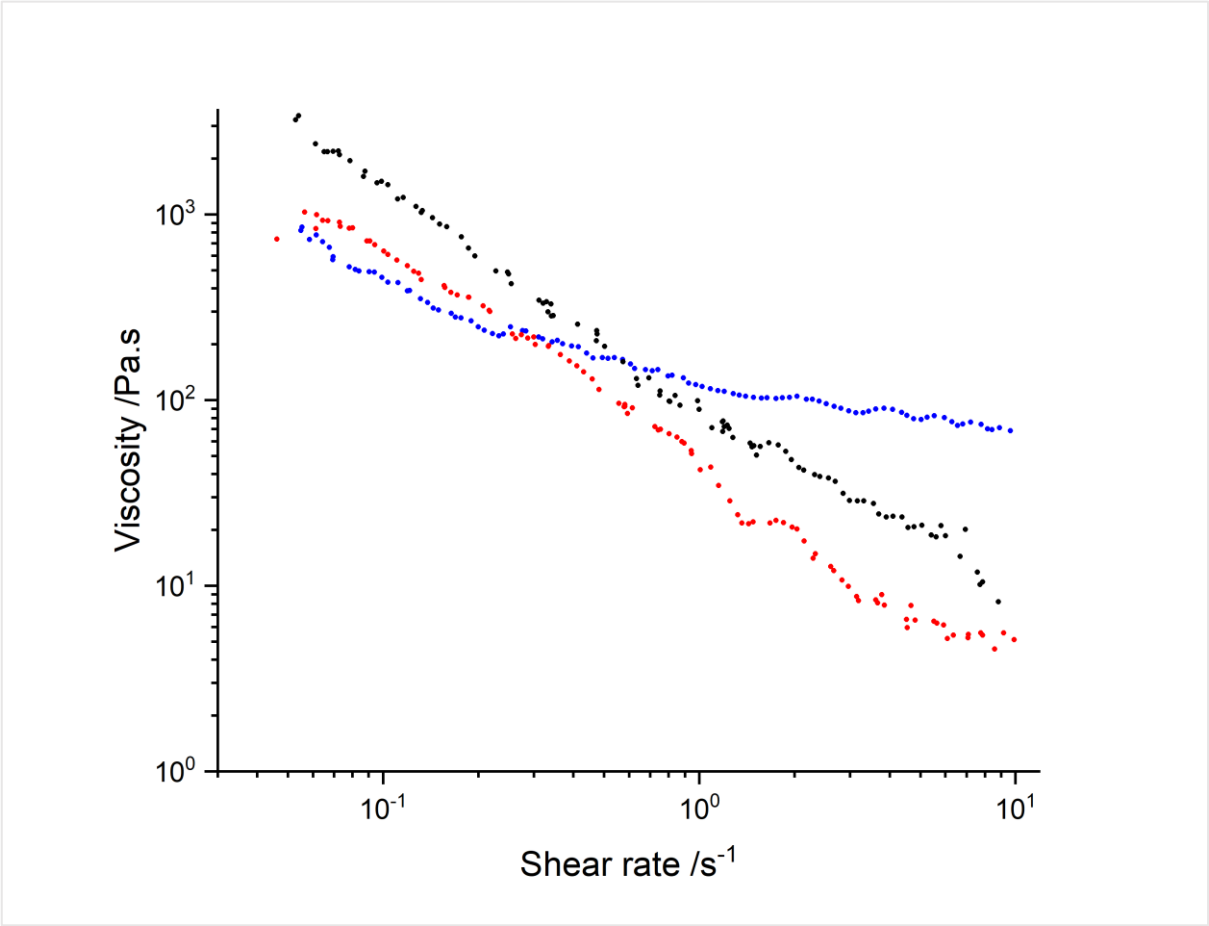

Figure S2. Thixotropic analysis of UiO-66 ink (black), polymer binder(acrylates) and UiO-66 MOF in ethanol (red) on a viscosity (Pa·s) over shear rate (s^{-1}) log-log graph

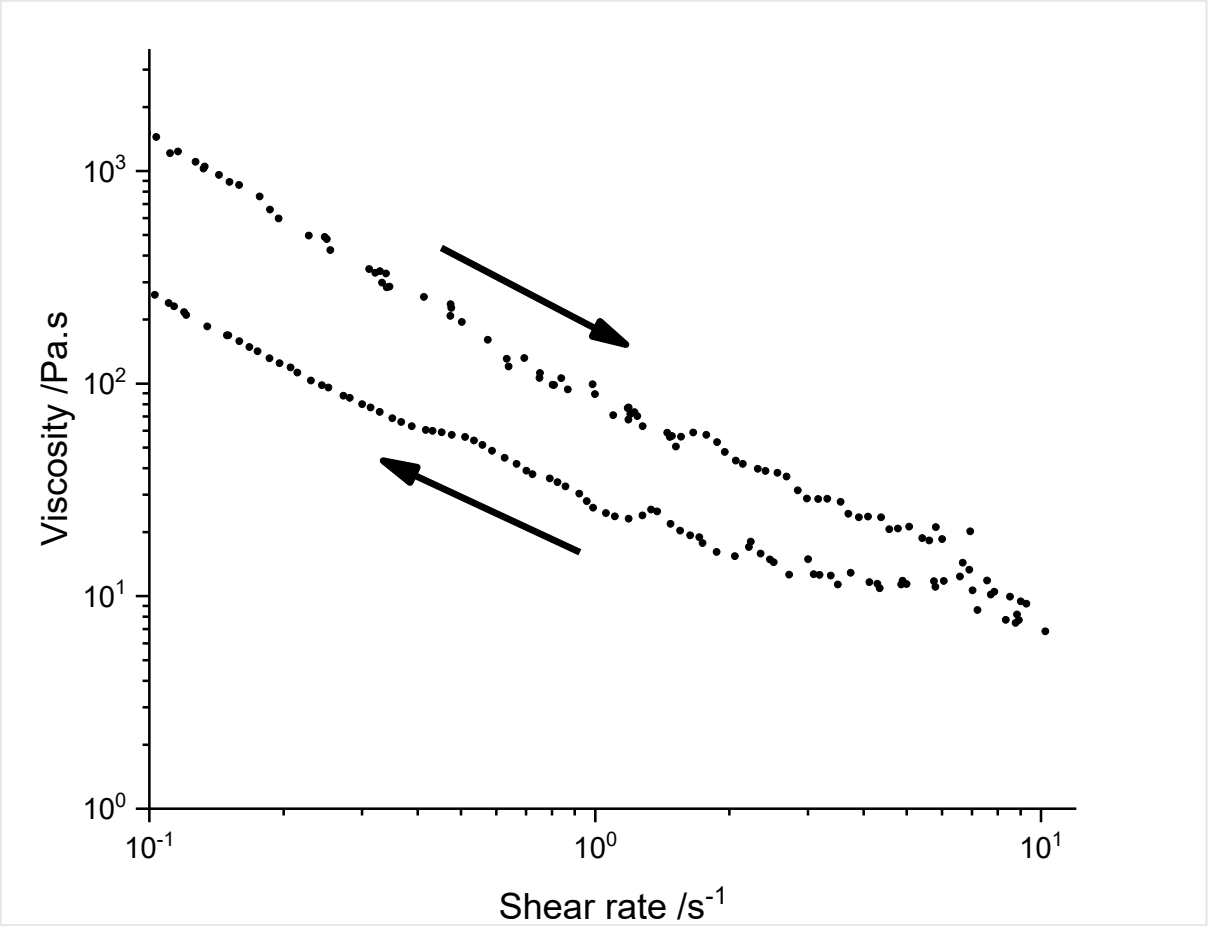

Figure S3. Log-log graph of viscosity (Pa·s) of UiO-66 composite ink against shear rate(s^{-1}).

3.3. Fourier Transform Infrared Spectroscopy– Attenuated Total Reflectance, FTIR-ATR

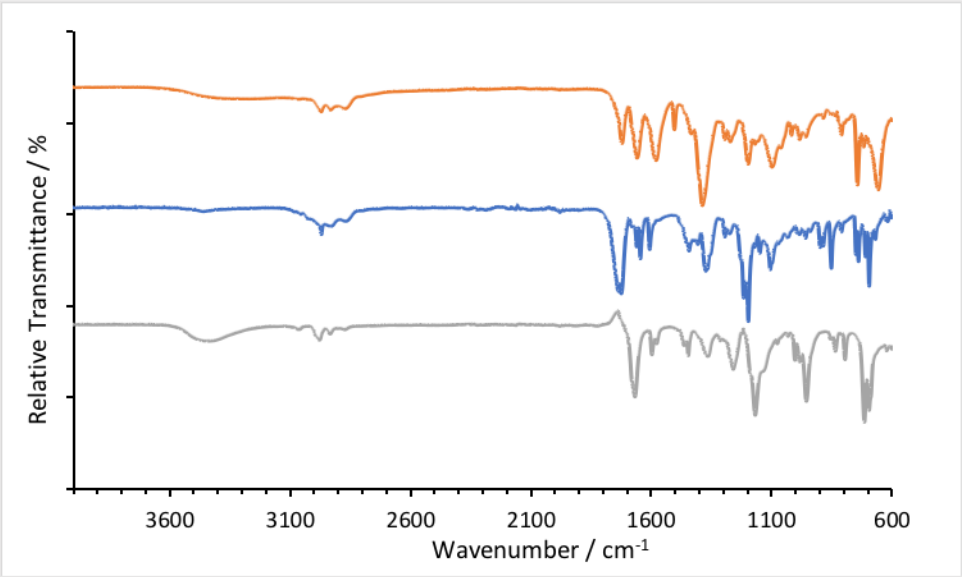

Figure S4. FT-IR spectra of photoinitiators 2-hydroxy-2-methylpropiophenone (orange) and phenylbis(2,4,6-trimethylbenzoyl) phosphine oxide (grey) as well as a mixture of 2-hydroxy-2-methylpropiophenone and phenylbis(2,4,6-trimethylbenzoyl) phosphine oxide in a 80:20 wt% ratio (blue).

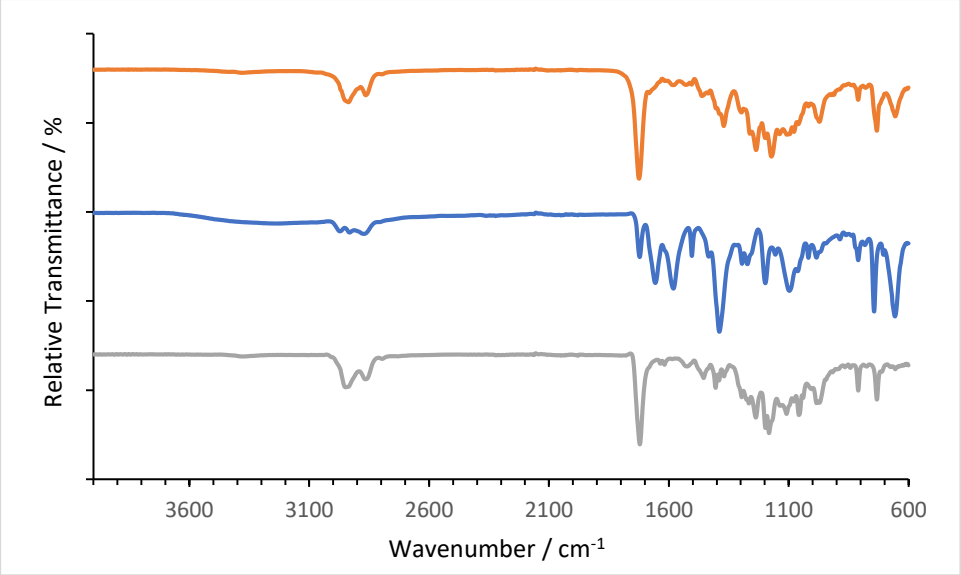

Figure S5. FT-IR spectra of the two acrylate binders TMPPTA (blue), Ebecryl®8413 (grey) and a mixture of both 23:77 wt.% (TMPPTA:Ebecryl®8413) used within the formulation (orange); samples measured are pre-cured samples.

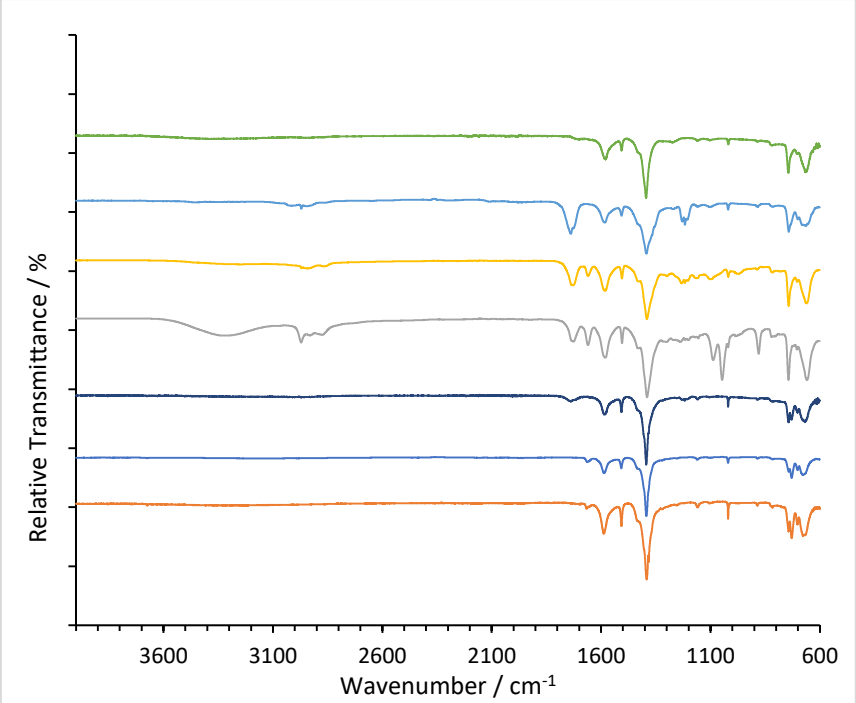

Figure S6. FT-IR spectra of the UiO-66 MOF (orange), UiO-66 MOF_{Δ} (blue), UiO-66 $MOF_{\Delta\text{-hyd}}$ (dark blue), UiO-66 ink (grey), UiO-66comp(yellow) and UiO-66$comp_{\Delta}$(light blue), UiO-66$comp_{\Delta\text{-hyd}}$ (green); all samples show that the structure of UiO-66 is retained. The loss of the vinyl frequency at around 2900 cm^{-1} indicates the successful polymerisation of the ink.

3.4. Nitrogen physisorption analysis (-196 °C)

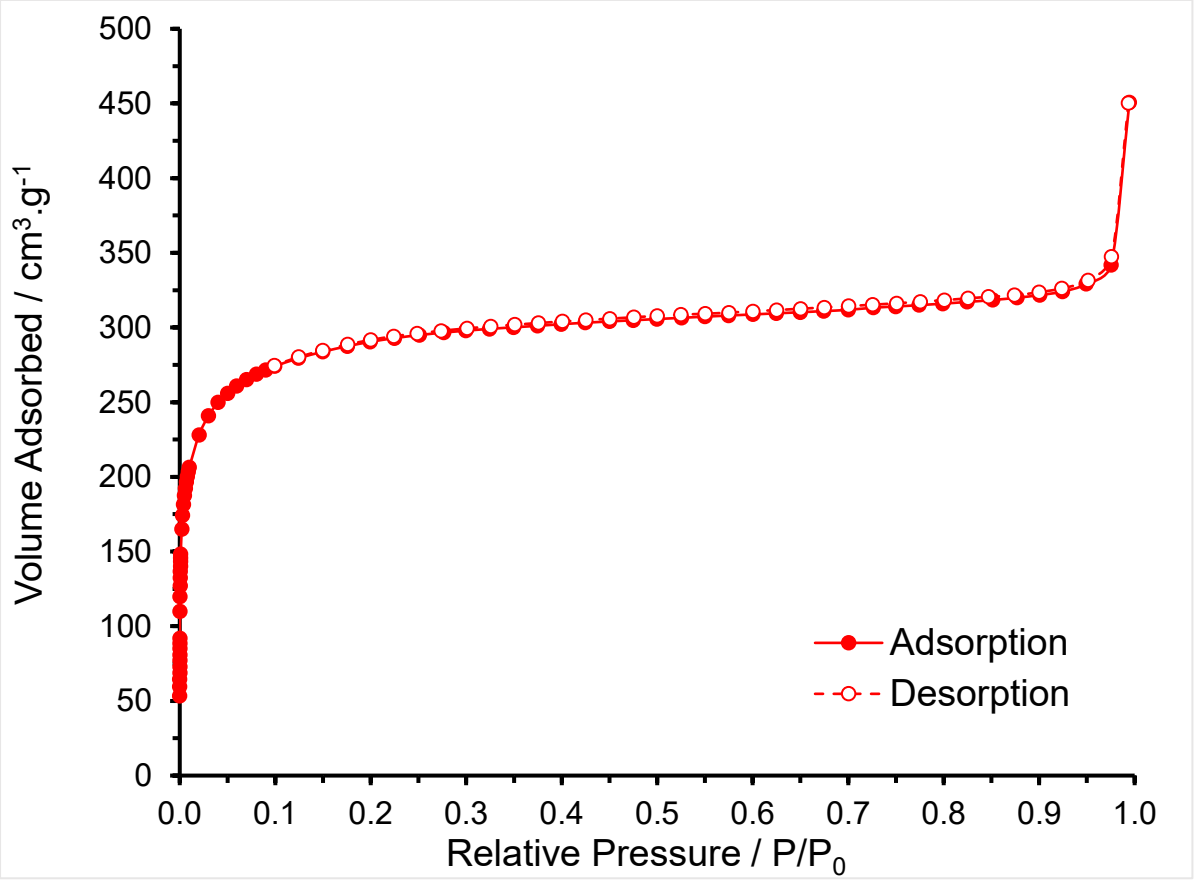

Figure S7. N_2 physisorption isotherm (- 196 °C) for the UiO-66 MOF.

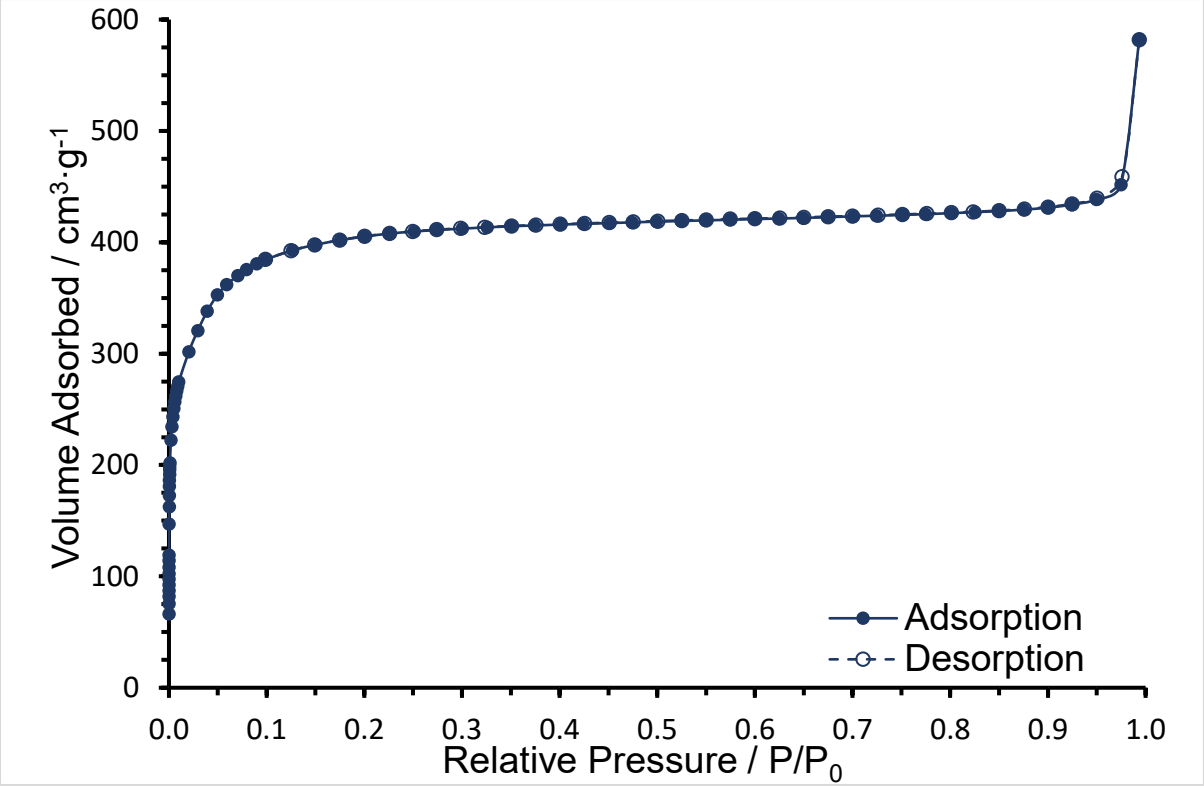

Figure S8. N_2 physisorption isotherm (- 196 °C) for the UiO-66 MOF_{Δ}.

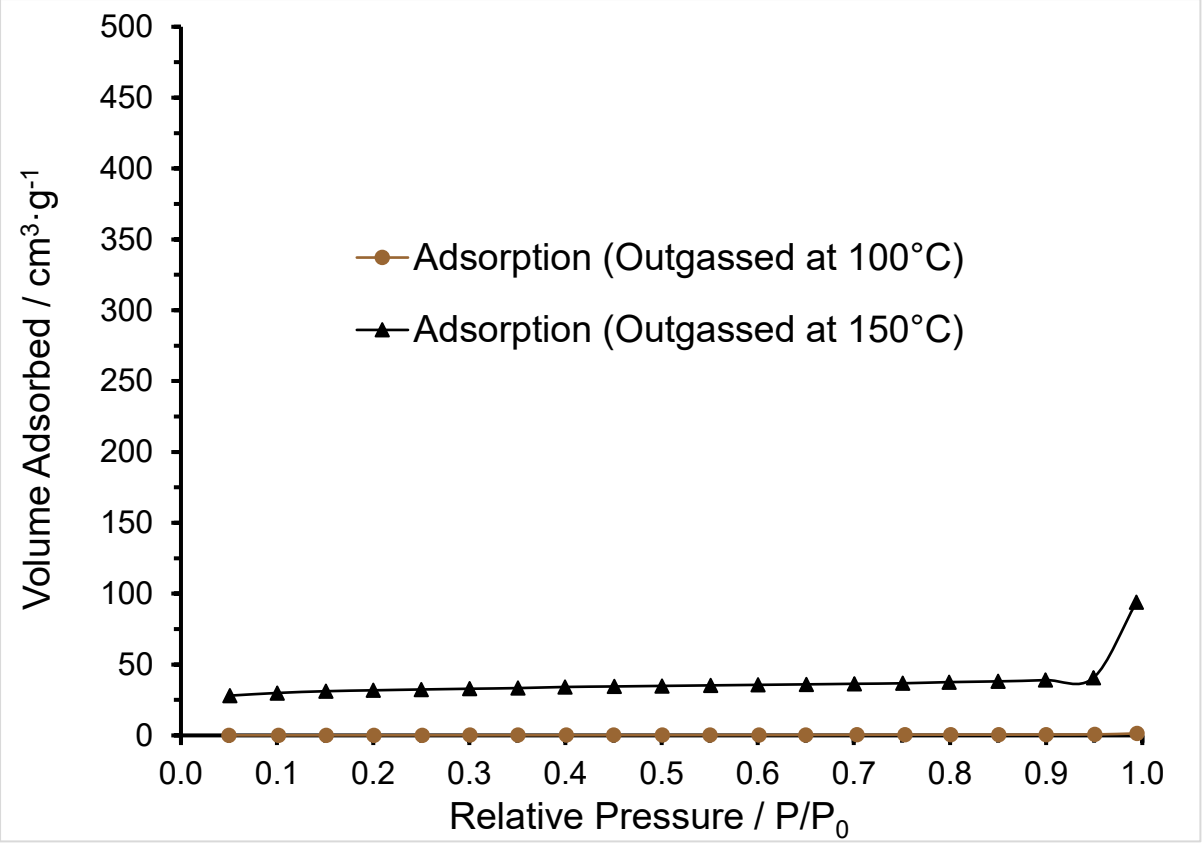

Figure S9. N_2 physisorption isotherms (- 196 °C) of as-printed UiO-66comp samples outgassed at 100 °C (brown) and 150 °C (black) for 12 hours.

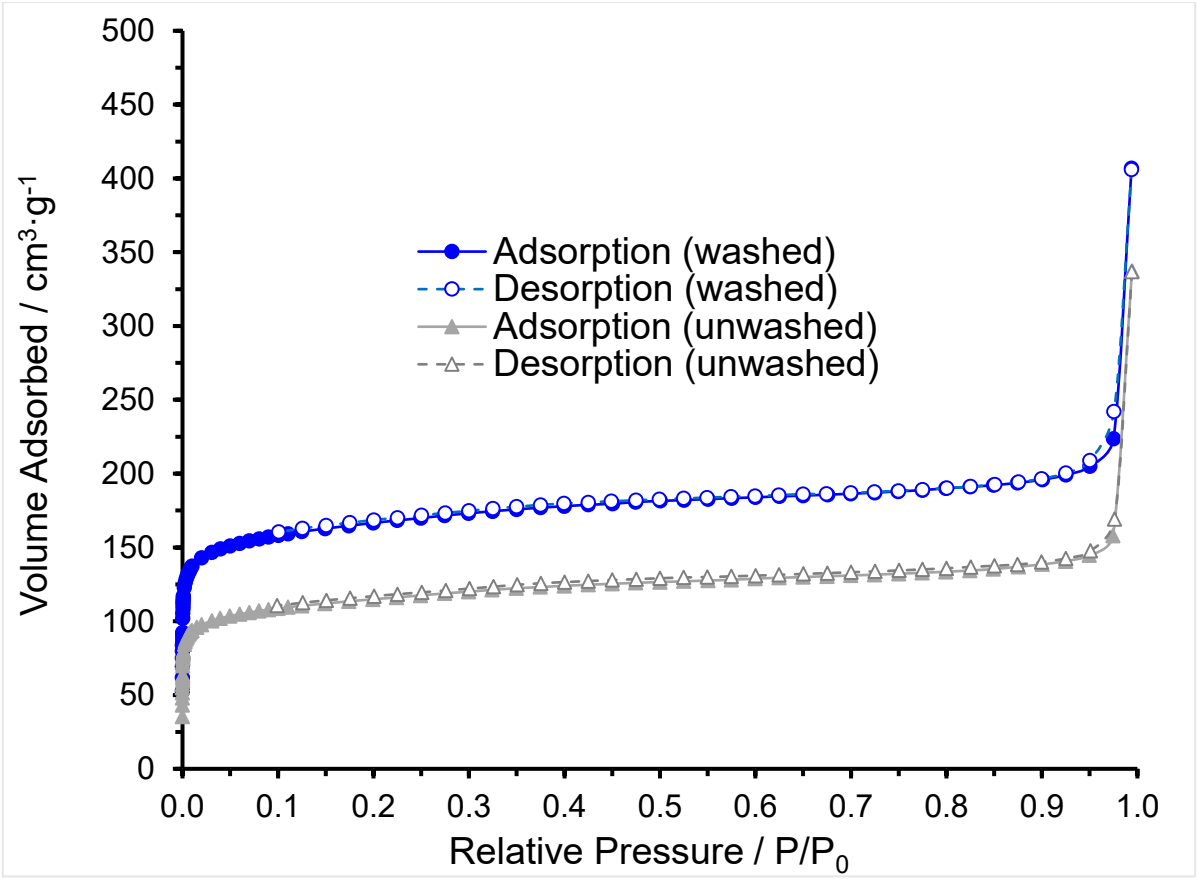

Figure S10. N_2 physisorption isotherms (- 196 °C) of UiO-66comp$_\Delta$ unwashed (grey) and washed (blue) samples.

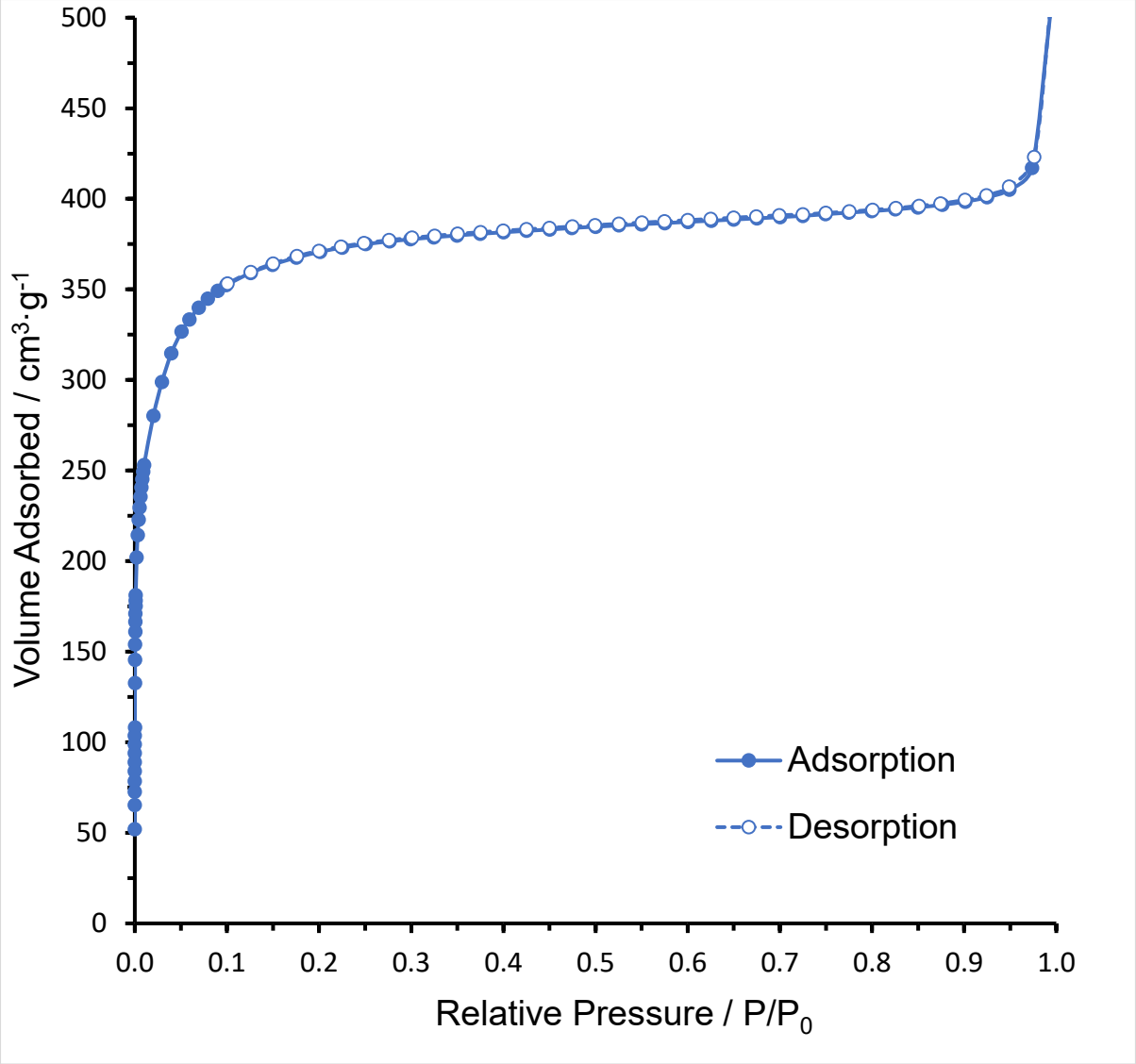

Figure S11. N_2 physisorption isotherm (- 196 °C) for the UiO-66$_{\Delta\ hyd}$.

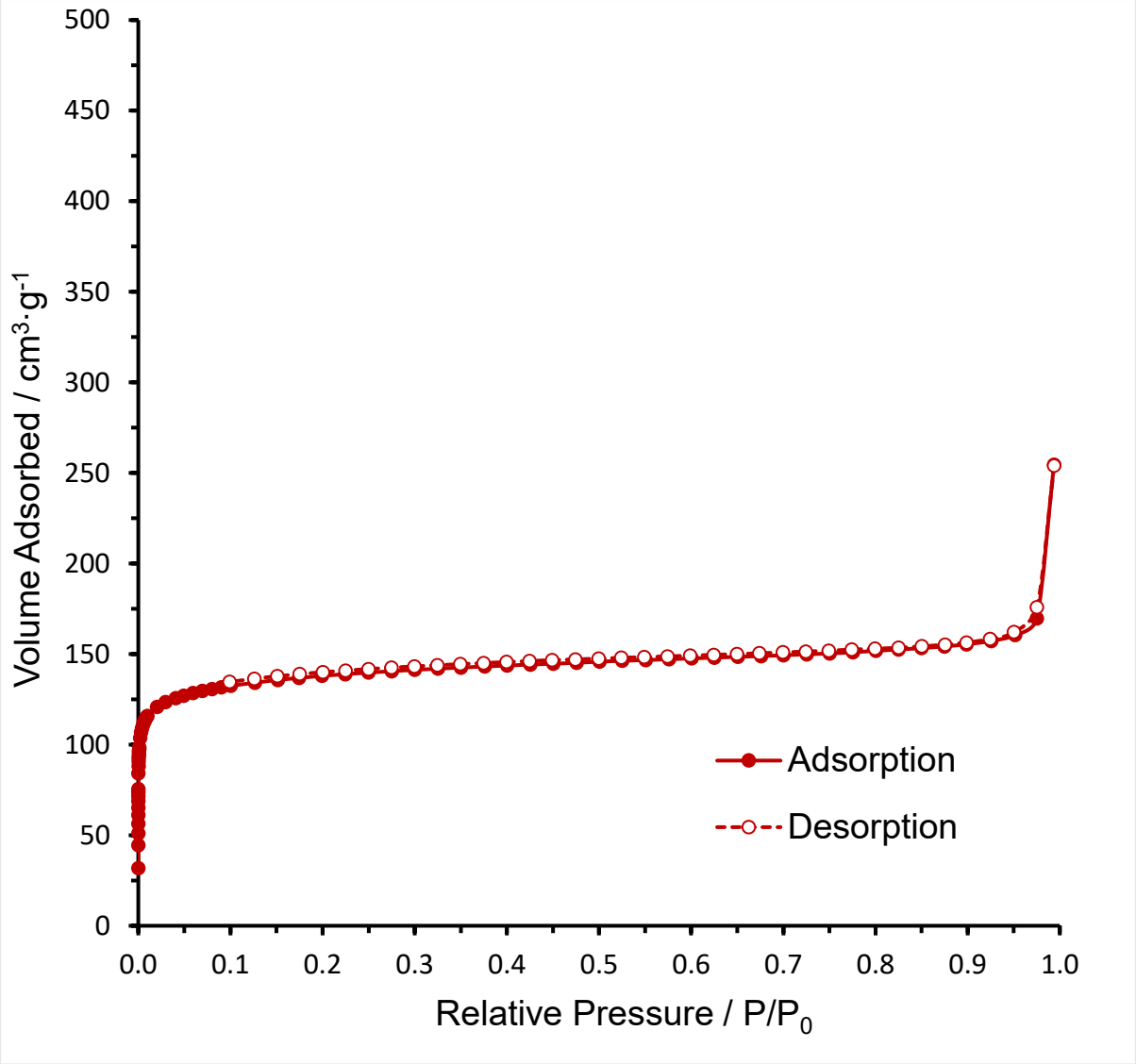

Figure S12. N_2 physisorption isotherm (- 196 °C) for the UiO-66comp$_{\Delta\ hyd}$.

Table S1: Physicochemical data extracted from N_2 physisorption experiments (- 196 °C).

	S_{BET} ($m^2 \cdot g^{-1}$)	NLDFT Pore Width (nm)	V_p ($cm^3 \cdot g^{-1}$)	NLDFT V_{micro} ($cm^3 \cdot g^{-1}$)	T-plot V_{micro} ($cm^3 \cdot g^{-1}$)
UiO-66 MOF	1106	1.1	0.51	0.33	0.39
UiO-66$_{\Delta}$	1590	1.1	0.68	0.67	0.57
UiO-66comp (outgassed 100 °C)	0.5	-	-	-	-
UiO-66comp (outgassed 150 °C)	100	-	0.06	0.03	0.04
UiO-66$_{\Delta \cdot hyd}$	1447	1.1	0.63	0.42	0.50
UiO-66comp$_{\Delta}$ unwashed	434	1.1	0.22	0.14	0.14
UiO-66comp$_{\Delta}$ washed	633	1.1	0.32	0.20	0.21
UiO-66comp$_{\Delta \cdot hyd}$	533	1.1	0.25	0.18	0.18

3.5. Thermogravimetric Analysis, TGA

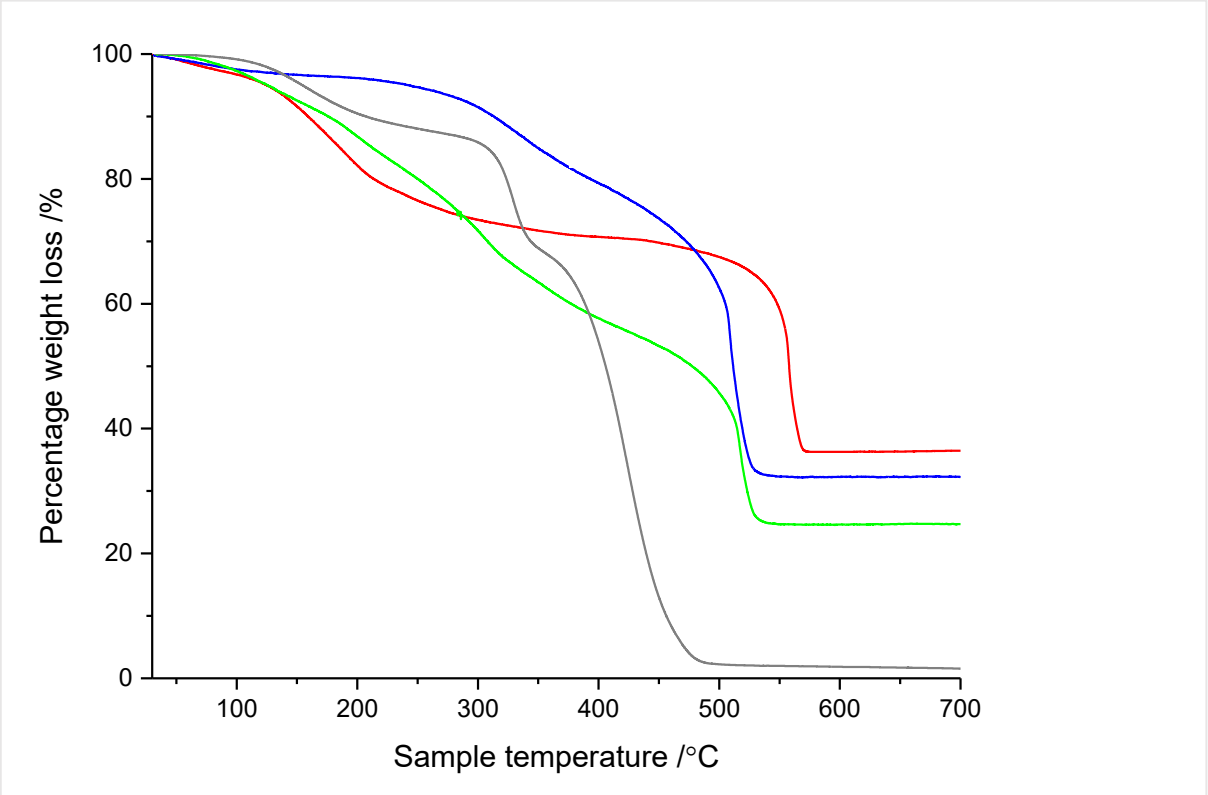

Figure S13. TGA curve between 30-700 °C under an airflow (30 mL min^{-1}) of the UiO-66 MOF (red), UiO-66comp$_{\Delta}$ (blue), UiO-66comp (green) alongside the resin mixture (grey).

TGA of the UiO-66 MOF (red) exhibits a loss of water and dehydration of hydroxyl groups, up to approximately 300 °C. Decomposition of the UiO-66 framework starts at 500 °C whereby the organic ligand is decomposing and stable and inert ZrO_2 (35 wt%) is formed. Therefore, the zirconium content of UiO-66 can be calculated to be 25.9 wt%.

UiO-66comp (green) exhibited a weight loss up to 400 °C, indicative of physisorbed water from the UiO-66 and the loss of all polymer binder. The remaining percentage weight, assigned to residual ZrO_2, is obtained at 24 wt% thus the final zirconium content of 17.8 wt% can be calculated.

UiO-66comp$_{\Delta}$ (blue) displayed a weight loss up to 400 °C. This weight loss can be attributed to the loss of water that was adsorbed during sample cooling in air. Residual ZrO_2 is 32 wt%, thus the final zirconium content of 23.7 wt% can be calculated.

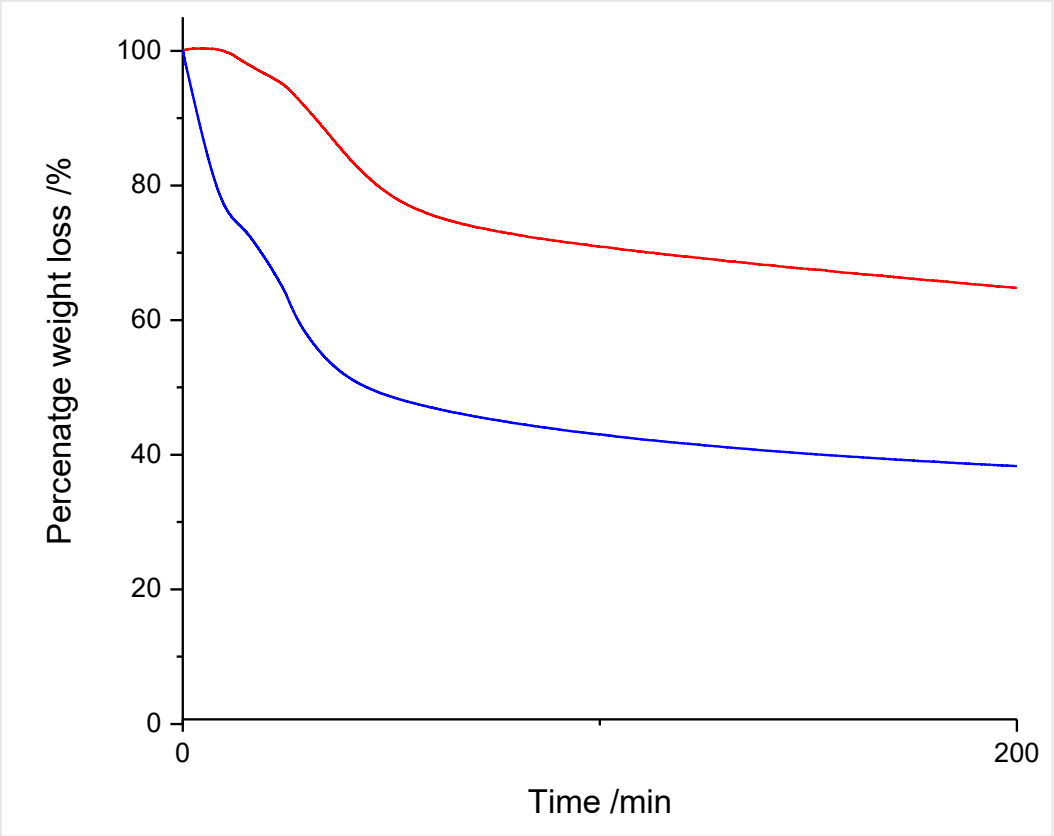

Figure S14. TGA isotherm plot at 280 °C for 200 min under an airflow (30 mL min^{-1}) of the UiO-66 MOF (red) and the UiO-66comp (blue).

Isothermal gravimetric analysis of the UiO-66 MOF was undertaken to show the stability and retention of the crystallographic structure, during thermal exposure at 280 °C. For the UiO-66 MOF sample, it can be seen that approximately 20% weight loss occurs within the first 60 min. This is largely attributed to the loss of physisorbed water, dehydroxylation of the $ZrO_4(OH)_2$ clusters,[2] and partial decomposition of excess ligands in pores, and the linkers within the MOF structure, as supported by the work of Shearer *et al.*[3] Additionally, it was found by PXRD that the UiO-66 MOF retained its crystallographic structure up to 280 °C (See Figure 2).

3.6. ICP-OES

Table S2: ICP-OES data showing zirconium content.

	Zr /%
UiO-66 MOF	30.829
UiO-66 MOF_{Δ}	30.389
UiO-66comp	17.107
UiO-66$comp_{\Delta}$	22.446
UiO-66$comp_{\Delta.hyd}$	22.651

Samples were digested with aqua regia followed by HCl treatment at 170 °C in a microwave reactor. Zirconium content obtained through ICP-OES analysis is in good agreement with the zirconium content calculated by TGA analysis.

Calculation of MOF content for catalysis using UiO-66comp and UiO-66$comp_{\Delta}$ is based on the Zr% obtained experimentally via ICP-OES for UiO-66 MOF_{Δ}, rather than on the assumed molecular formula of UiO-66, due to the well-known structural defects that UiO-66.

3.7. Catalysis

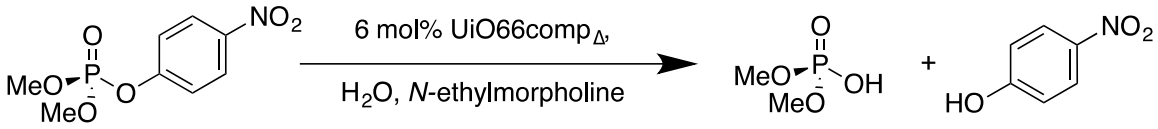

Figure S15. Scheme illustrating hydrolysis of methyl-paraoxon into dimethoxyphosphine oxide and p-nitrophenol, catalysed by UiO-66$comp_{\Delta}$.

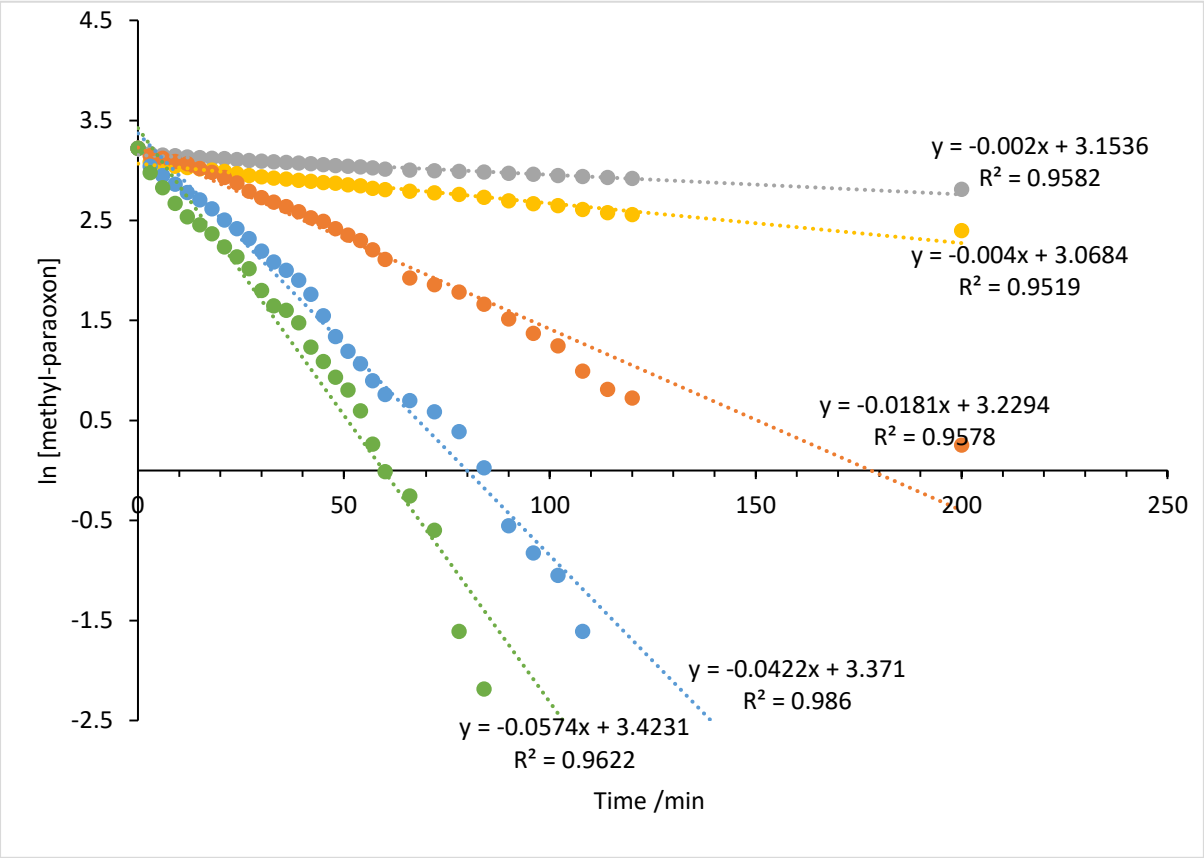

Figure S16. Kinetic measurements of catalytic hydrolysis of methyl-paraoxon in the presence of UiO-66 MOF_{Δ} (grey), UiO-66 $MOF_{\Delta\cdot hyd}$ (gold), activated UiO-66 MOF (green), UiO-66$comp_{\Delta}$ (orange) and UiO-66$comp_{\Delta\cdot hyd}$ (blue). Respective plots of ln[c] vs time (min), [c] = concentration of residual agent (mM) r^2>0.95.

Turnover frequency calculation

Turnover frequency = TOF

Turnover number = TON

$$TON = \frac{mols\ product}{mols\ catalyst}$$

Mols of catalyst* = 0.045 mol%[4]

$$TOF = \frac{TON}{time\ (s)}$$

Calculations taken after 30 minutes (1800 seconds)*

* Based on assumptions that ca. 0.045 mol% of catalyst loading (corresponding to surface sites) are catalytically active, and the time point chosen due to similar calculations reported by Katz *et al.*[4,5]

Half-life (mins)

$$Half - life = \frac{\ln(2)}{-m}$$

m = gradient of kinetic graphs (Figure S15)

Table S3. Catalytic activity of the tested samples.

*based on the assumption that ca. 0.045 mol% of catalyst loading (corresponding to surface sites) are catalytically active sites.[4,5]

Samples	Initial rate (mM s^{-1})	TON	TOF (s^{-1})	Half-life (mins)
UiO-66	0.0133	1684.4	0.94	12.1
UiO-66$_{\Delta}$	0.0021	262.2	0.15	346.6
UiO-66$_{\Delta\cdot hyd}$	0.0045	548.9	0.30	173.3
UiO-66comp$_{\Delta}$	0.0049	864.4	0.48	38.3
UiO-66comp$_{\Delta\cdot hyd}$	0.0105	1426.6	0.79	16.4

3.8. Nuclear Magnetic resonance, NMR

Data Analysis.

The percentage hydrolysis at each time point was determined by dividing the $^{31}P\{^{1}H\}$-NMR integral(s) of the signal(s) of the hydrolysis products by the sum of all $^{31}P\{^{1}H\}$ integrals (and multiplying by 100). The time point values were defined as the time of measurement start plus 1.5 minutes (total measurement time per time point was 3 minutes).

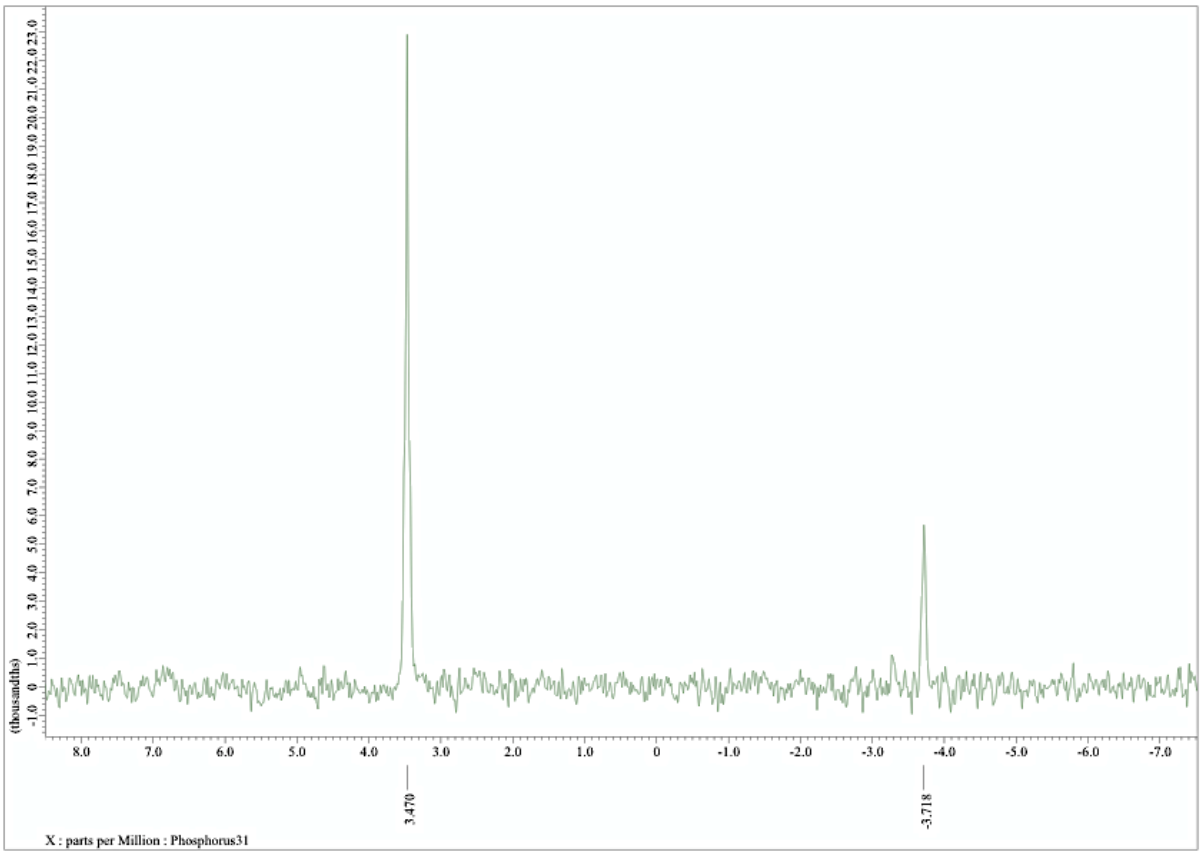

Figure S17. $^{31}P\{^{1}H\}$-NMR spectrum of methyl paraoxon after 200 minutes of catalysis using UiO-66 MOF. The peak at -3.72 ppm is unreacted methyl paraoxon. The peak at 3.47 ppm is the desired hydrolysis product (dimethyl phosphate).

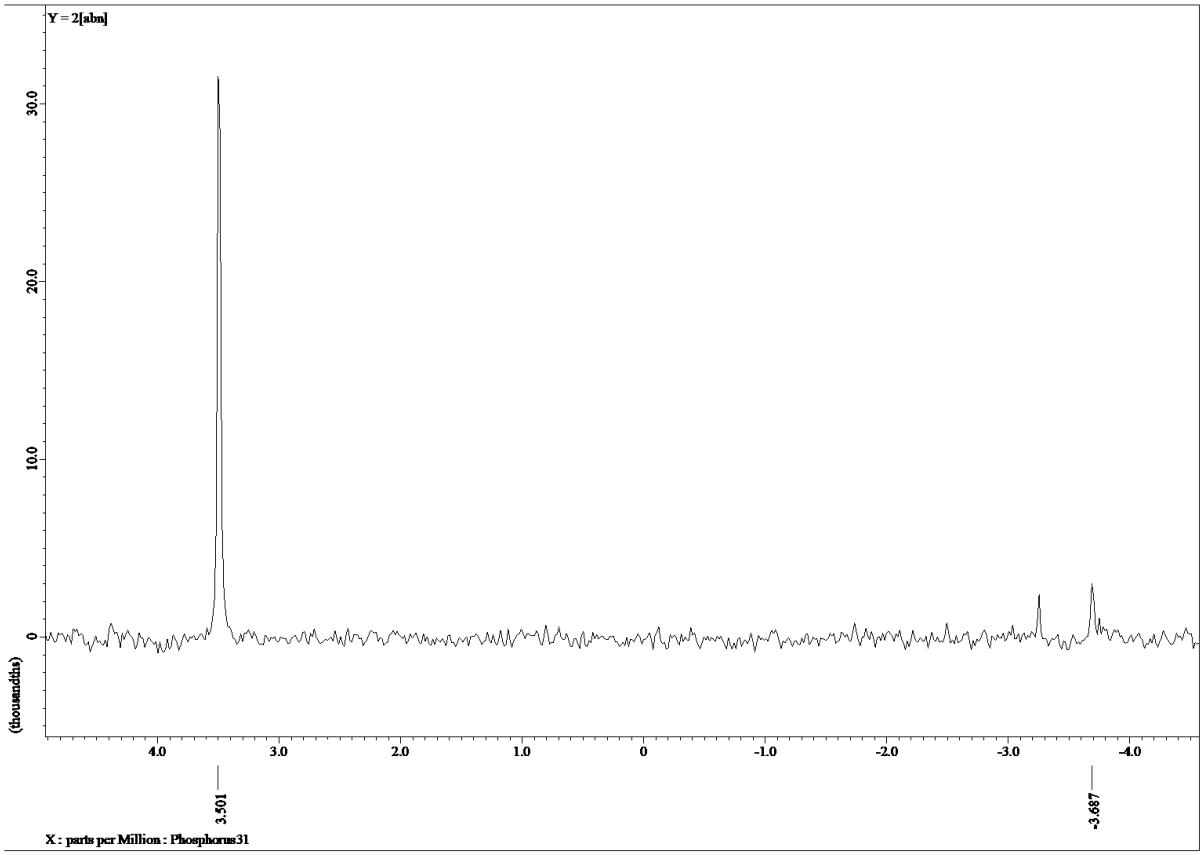

Figure S18. $^{31}P\{^{1}H\}$-NMR spectrum of methyl paraoxon after 200 minutes of catalysis using UiO-66comp$_{\Delta}$. The major peak represents the desired hydrolysis product (dimethyl phosphate).

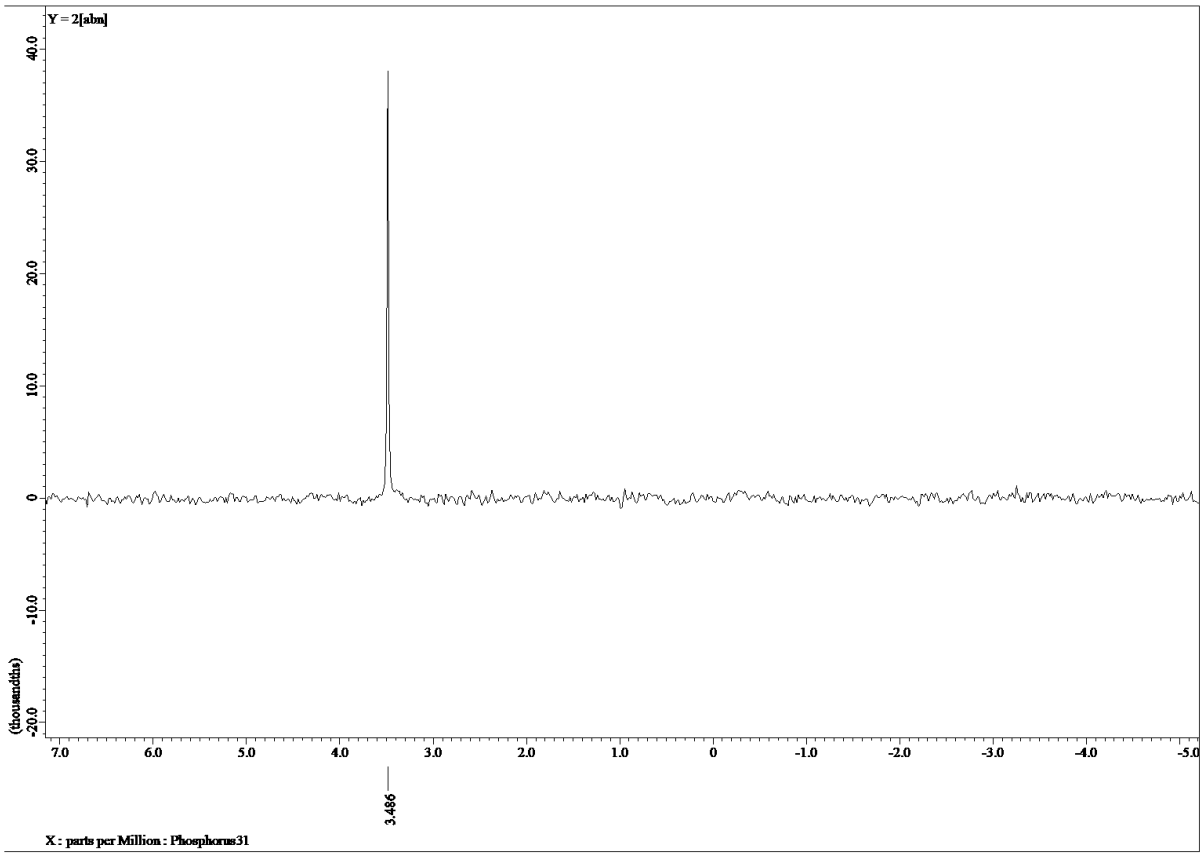

Figure S19. $^{31}P\{^{1}H\}$-NMR spectrum of methyl paraoxon after 200 minutes of hydrolysis catalysis using UiO-66comp$_{\Delta.hyd}$ showing negligible amounts of methyl paraoxon remaining.

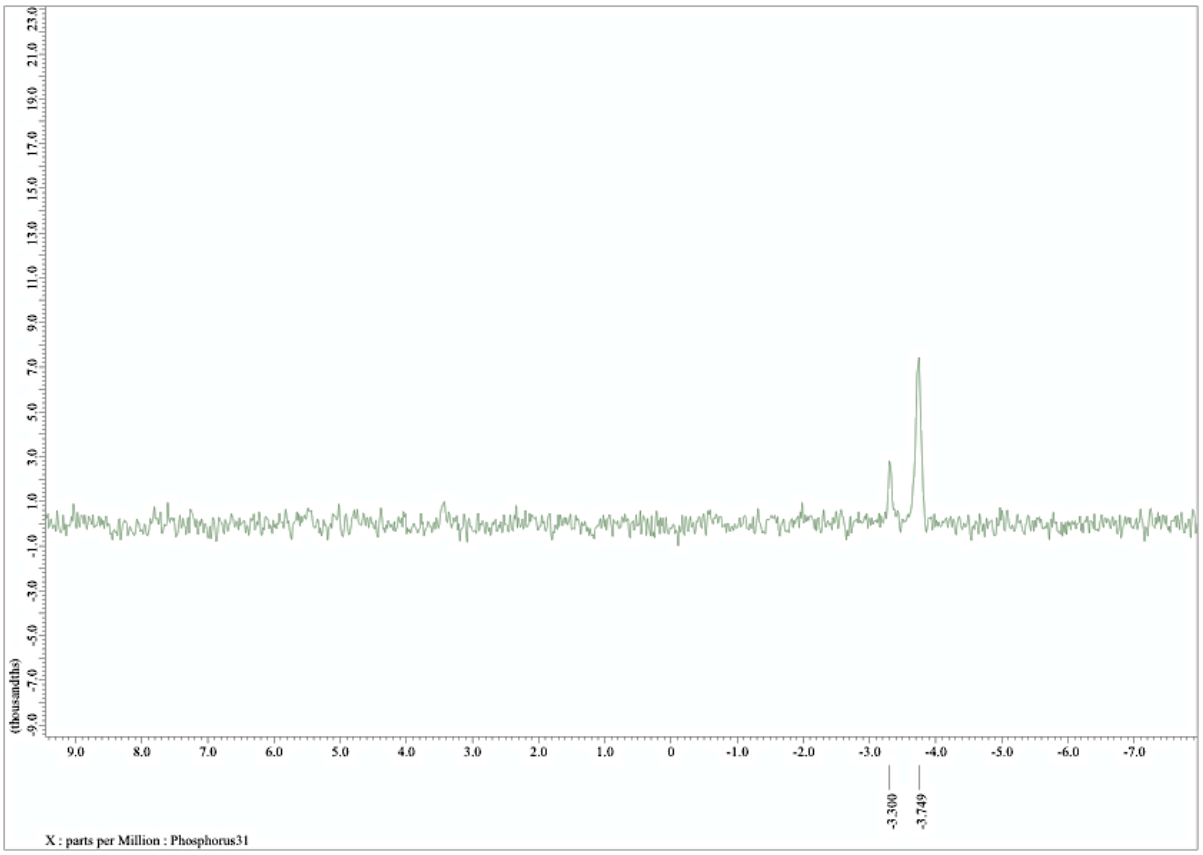

Figure S20. ^{31}P NMR of methyl paraoxon after 200 minutes of self-hydrolysis without any MOF catalyst. The peak at -3.745 ppm is unreacted methyl paraoxon. The peak at -3.30 ppm is a hydrolysed phosphonate compound, methyl 4-nitrophenyl phosphate. [3,6]

3.9. Mechanical testing

Preparation of composites for mechanical testing

To obtain indicative values of material compression strengths, monoliths of the resin mixtures and UiO-66 composite mixtures were formed via syringe molding. This allowed the avoidance of stress concentration effects arising from the shape and structure of 3D prints. A resin mixture of PI blend (0.38 g), Ebecryl® 8413 (3.27 g) and TMPPTA (0.96 g) was homogenized (10,000 rpm, 3 minutes). The resulting mixture was then placed into 2 mL NORM-JECT® syringes. The syringes were then placed under a 365 nm UV light (5 cm working distance) with a steady stream of N_2 and irradiated 4 times for ten minutes, with the syringes flipped each time to ensure even curing. The plunger was then removed and the syringe was carefully cut away from the molded resin monoliths using pliers. The resulting resin monoliths were cut to size using a rotary dremel diamond blade.
The same procedure was used in the preparation of the MOF composite samples for mechanical testing, using the same formulation as for 3D printed UiO-66 composites.
Monoliths which were heat treated prior to mechanical testing underwent the same procedure as outlined for the heat treated UiO-66comp.

Table S4: Mechanical testing data for binder mixture (pre-furnace), resin (post furnace), MOF composite (pre-furnace) and MOF composite (post furnace). As it was not possible to ensure perfectly even UV-curing of the composites, the data should be taken as indicative lower estimates of the composites' mechanical properties.

	Compression Strength (MPa)	Young's Modulus (MPa)
Resin mixture (pre-furnace)	20.0 ± 0.4	26 ± 2
Resin mixture (post furnace)	4.4 ± 0.7	13 ± 6
UiO-66 composite (pre-furnace)	22.4 ± 0.8	24 ± 2
UiO-66 composite (post furnace)	4.9 ± 0.9	31 ± 5

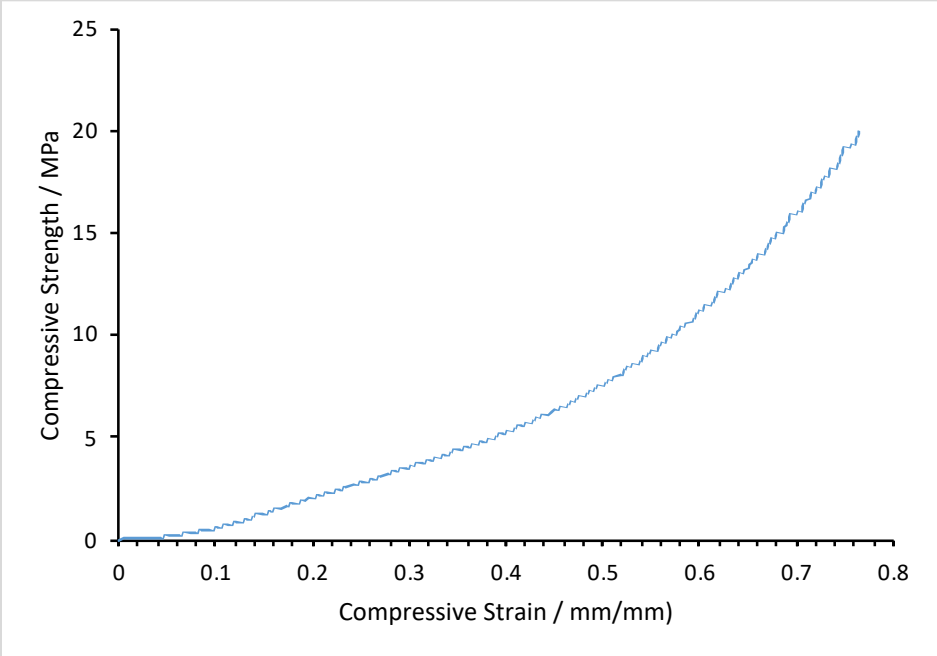

Figure S21. Stress-strain curve of resin pre-furnace resin mixture only. Limit of the equipment was reached before the break point was observed.

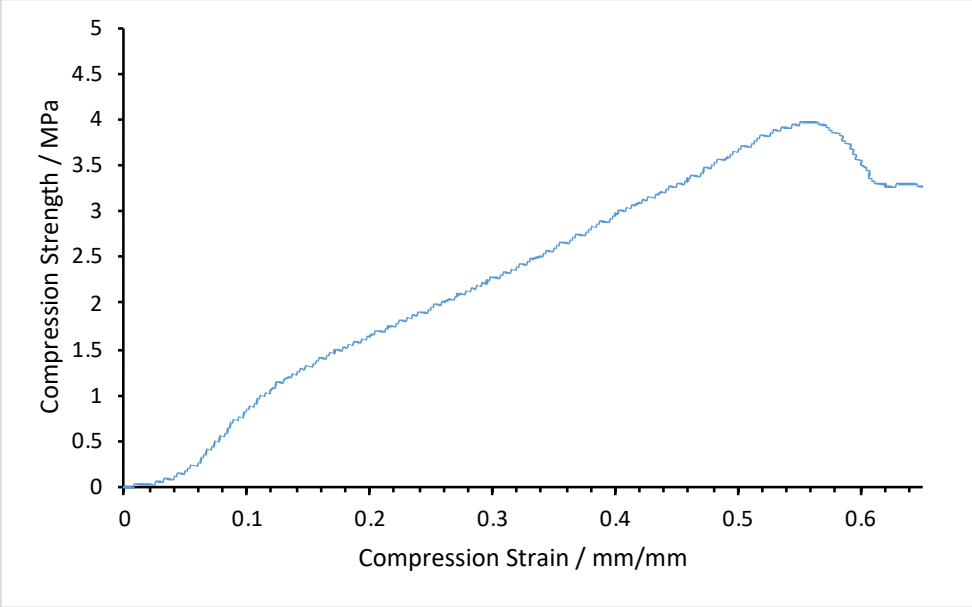

Figure S22. Stress-strain curve of thermally treated resin mixture.

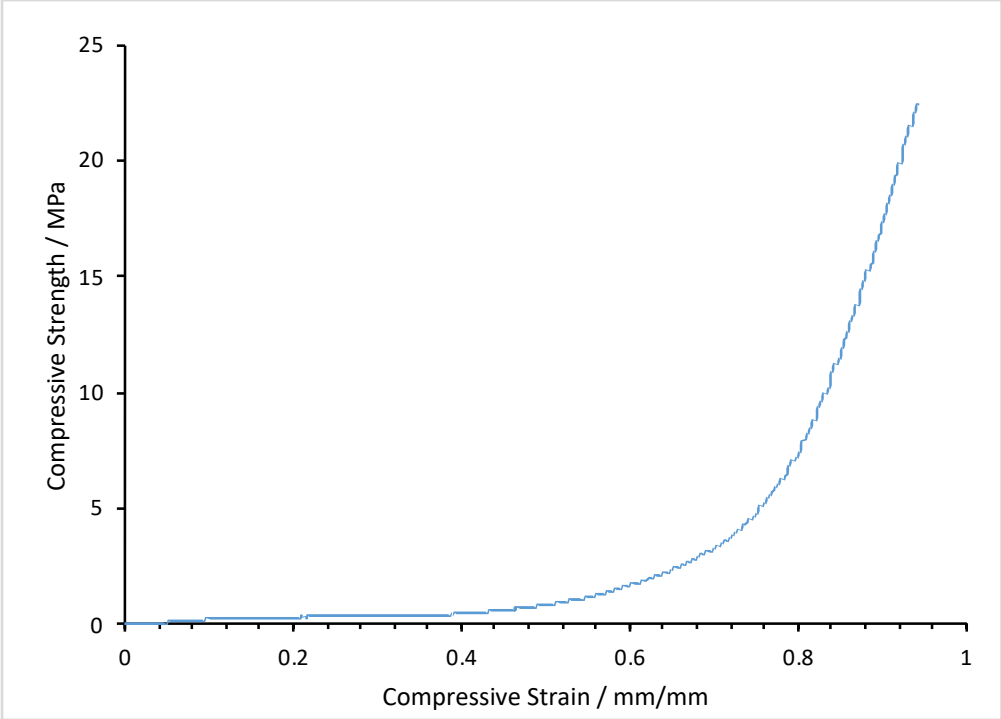

Figure S23. Stress-strain curve of UiO-66comp. Limit of the equipment was reached before the break point was observed.

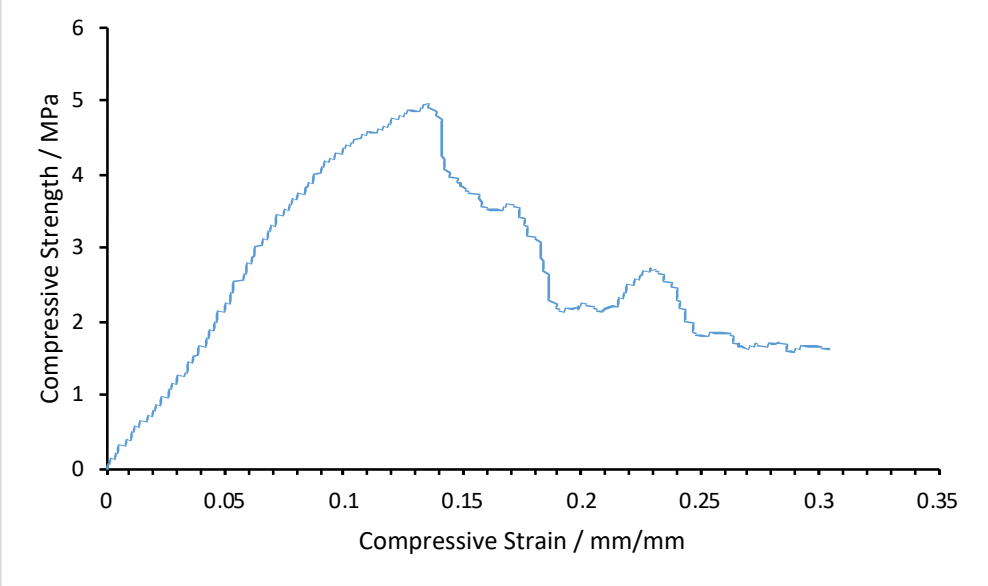

Figure S24. Stress-strain curve of UiO-66comp$_{heat}$. The material becomes more brittle after thermal treatment.

3.10. Optical photographs of samples

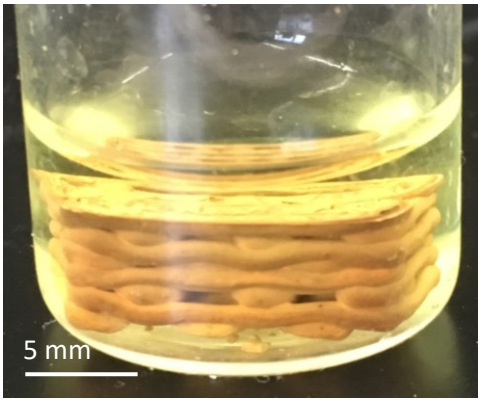

Figure S25. Photograph of MOF composite (furnaced) in an aqueous solution of ethylmorpholine and paraoxon after 2 months, no structural damage or deterioration observed by visual inspection.

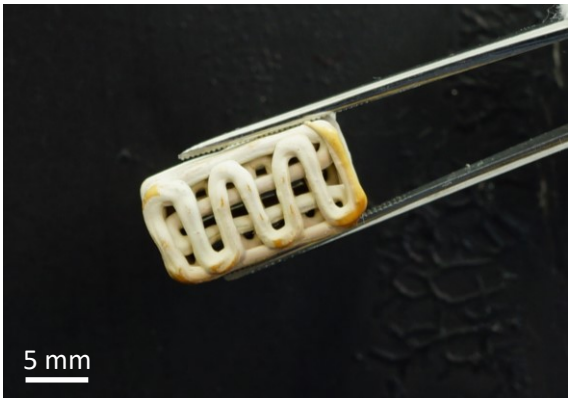

Figure S26. Photograph of MOF composite (furnaced) removed from the above solution (Figure S20). The composite can be easily handled with tweezers without especial care – no damage is observed with normal handling, even after heat treatment and prolonged soaking in aqueous solutions.

Figure S27. Photograph of MOF UiO-66 before (a) and after (b) heating at 280 ^{o}C for 30 minutes. A faint darkening of the MOF can be observed.

4. References

1 M. J. Katz, Z. J. Brown, Y. J. Colón, P. W. Siu, K. A. Scheidt, R. Q. Snurr, J. T. Hupp and O. K. Farha, *Chem. Commun.*, 2013, **49**, 9449–9451.

2 F. Vermoortele, R. Ameloot, A. Vimont, C. Serre and D. De Vos, *Chem. Commun.*, 2011, **47**, 1521–1523.

3 G. C. Shearer, S. Chavan, J. Ethiraj, J. G. Vitillo, S. Svelle, U. Olsbye, C. Lamberti, S. Bordiga and K. P. Lillerud, *Chem. Mater.*, 2014, **26**, 4068–4071.

4 M. J. Katz, J. E. Mondloch, R. K. Totten, J. K. Park, S. T. Nguyen, O. K. Farha and J. T. Hupp, *Angew. Chemie Int. Ed.*, 2014, **53**, 497–501.

5 M. J. Katz, S. Y. Moon, J. E. Mondloch, M. H. Beyzavi, C. J. Stephenson, J. T. Hupp and O. K. Farha, *Chem. Sci.*, 2015, **6**, 2286–2291.

6 X. Liao, P. S. R. Anjaneyulu, J. F. Curley, M. Hsu, M. Boehringer, M. H. Caruthers and J. A. Piccirilli, *Biochemistry*, 2001, **40**, 10911–10926.